01

MHD stirrers for machines of continuous casting of cylindrical ingots

© S.Yu. Khripchenko, E.Yu. Tonkov

Institute of Continuous Media Mechanics, Ural Branch, Russian Academy of Sciences,

614013 Perm, Russia

e-mail: tonkov.e@icmm.ru, khripch@icmm.ru

Received January 13, 2025 Revised March 19, 2025 Accepted March 25, 2025

Modern trends in the development of the aviation and aerospace technology suggest the necessity of constant expansion of the production capacity of both manufacturing plants and raw material suppliers. Aluminum and aluminum alloys are among the preferred metals in this field of industry. The use of MHD stirrers is advantageous for manufacturing cylindrical ingots from aluminum and aluminum alloys during the continuous casting process. By setting specific liquid metal stirring flow parameters, one can change the structure of ingots and produce high-quality ingots essential for designing high-performance products. In this regard, an urgent question arises about the dimensions of MHD stirrers that are needed to place a maximum number of crystallizers on a casting table. In this paper, we consider different designs of MHD stirrers for machines of continuous casting of aluminum ingots. The goal is to compare the efficiency of these devices by analyzing the electromagnetic fields produced by stirrers in liquid metal using mathematical modeling techniques. We also present a fundamentally new design scheme of a rotating magnetic field inductor with inclined core poles. The application of this inductor helps to significantly decrease the dimensions of MHD stirrers, to place a sufficient amount of MHD stirrers and crystallizers on a casting table and to reduce the production costs of aluminum cylindrical ingots.

Keywords: MHD stirrer, travelling magnetic field inductor, rotating magnetic field inductor,, toroidal flow, poloidal flow, COMSOL Multiphysics, inclined poles.

DOI: 10.61011/TP.2025.08.61729.9-25

Introduction

Aluminum alloys have a high specific strength and a number of mechanical, operating and special properties, which is essentially important for automobile, aviation and aerospace engineering [1]. When producing round ingots from the mentioned materials, a crystallizer of a continuous casting machine has a dendrite structure formed at a front of crystallization of liquid metal, which predetermines low plastic properties of the produced ingots [1–3]. In order to improve the alloy properties during continuous casting, the so-called "warm top" is installed above the crystallizers of the continuous casting machine. The "warm top" (where the liquid metal is supplied from a furnace) covers an inductor of the MHD stirrer designed to stir the liquid metal in volume. The very crystallizer is below the "warm top", where the mixed metal solidifies and is pulled into the ingot.

When an azimuthal (toroidal) and meridional (poloidal) flow of liquid aluminum or its alloys is generated in the "warm top" there is effect on formation of the structure and distribution of impurities within a volume of the ingot being crystallized [4,5]. The toroidal flow directly affects formation of a fine-grained structure of the ingot. This flow at the crystallization front (which is below the "warm top" at an upper edge of the crystallizer) prevents formation of dendrites when diluting them during formation and creating many small centers of crystallization. The poloidal flow mainly ensures heat-mass transfer, thereby affecting a form

of crystallization front and distribution of the impurity across the ingot volume.

As shown by the experiments, in liquid metals, convective heat transfer substantially exceeds molecular heat transfer [6]. Therefore, availability of the poloidal flow enhances heat transfer from an upper part of the volume of the crystallizer's warm top (where liquid aluminum is continuously supplied) to the front of ingot crystallization. At the same time, it is possibly to effectively affect a geometry of the crystallization front by adjusting intensity of the flow and changing its direction [7]. It should be noted that the toroidal flow excited with the poloidal flow significantly reduces heat transfer by the poloidal flow [7].

When only the toroidal flow is excited in a liquid-metal cylinder, in a stationary mode, there is the so-called "solid-body" rotation within the volume of the "warm top" the difference from which will be observed in a small boundary layer near side walls (Fig. 1) and at the crystallization front, which complicates uniform distribution of various alloys components, impurities and inclusions across the volume. It is possible to correct the situation by making turbulent the entire volume of the "warm top" by the following methods: to arrange a reverse mode of the toroidal flow; to implement an intermittent mode of rotation; to excite the poloidal flow and the toroidal flow combined in the mixed volume [8–10].

The so-called two-directional stirring, when the poloidal flow is excited in addition to the toroidal flow, allows not only improving distribution of impurities and alloy

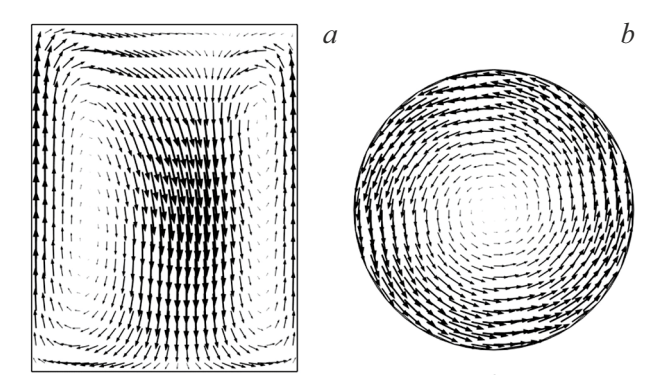


Figure 1. Nature of the flow as excited by a travelling (a) and a rotating (b) magnetic field (numerical calculation).

components within the metal volume, but also actively affect a form of the crystallization front during production of the ingot. A disadvantage of this method is that under simultaneous effect of the rotating and the travelling magnetic field there is their cross interaction that results in asymmetry of a resultant flow [11].

This situation may be corrected by feeding the inductors with currents, whose frequency is very different [11], or by arranging a time-alternate effect on the metal by these fields, which is structurally simpler and energetically more profitable [7].

When there are two inductors of the travelling and the rotating magnetic field in these stirrers, it increases their overall dimensions, which makes it difficult to place a required number of crystallizers on the same casting table of the continuous casting machine. Therefore, it is a relevant task to study various designs of MHD stirrers that create poloidal and toroidal stirring in the "warm top" and it is confirmed by intensification of research in this field in the industrialized countries.

1. Initial variant

The initial variant is a design that is schematically equivalent to the MHD stirrer which has two three-phase inductors of the rotating and the travelling magnetic field. This configuration was tested in domestic and foreign industrial sites and showed it efficiency both when affecting the structure of continuously cast round aluminum ingots and affecting distribution of impurities in their volume [3]. Geometrical sizes of the initial variant are shown in Fig. 2, a. The present study has considered several possible designs of the inductors of the MHD stirrers and compared their characteristics with characteristics of the three-phase MHD stirrer that was selected as the initial variant.

A working volume of the stirrer comprises a conducting cylinder (that models the "warm top" of the crystallizer with liquid aluminum), which has a diameter of 200 mm and a height that is equal to a height of the working volume

(Fig. 2, a). Electrical conductivity of the cylinder is equal to conductivity of liquid aluminum ($\sigma = 4.2 \cdot 10^6 \,\Omega^{-1} \,\mathrm{m}^{-1}$).

2. Two-phase inductors of the travelling and the rotating magnetic field

In order to improve efficiency of casting production, it is necessary to use several compactly arranged stirrers that are combined by the inductors into a single system. Application of the two-phase travelling magnetic field inductor makes it possible to reduce the height of the MHD stirrer [12,13]. The two-phase feeding diagram allows combining cores of the rotating magnetic field inductors of the adjacent MHD stirrers and thereby arranging them more compactly on the casting table of the continuous casting machine [14]. Therefore, the question arises about comparing efficiency of the considered MHD stirrer with the two-phase (Fig. 2, b) and the three-phase (Fig. 2, a) feeding diagram.

Toroidal rotation of the mixed liquid metal is caused by a moment of electromagnetic forces, which is created by the rotating magnetic field inductor, while poloidal motion of the metal is caused by a vortex nature of a vertical component of the electromagnetic forces that are created by the travelling field inductor of the MHD stirrer.

Comparison of the three-phase inductor of the travelling field with the two-phase inductor

Fig. 3 shows simplified layouts of the three-phase travelling field inductor and the two-phase travelling field inductor, which are computational models.

The efficiency of these designs was compared by a mean-square (across the volume) value of the azimuthal component of a rotor of the volume force ${\bf f}$ that has (as simplification) only a vertical component $(0, 0, f_z)$. Hereinafter, the axis Z coincides with a central axis of the liquid aluminum conducting cylinder and is directed along it; the axes X and Y are respectively within a plane that is normal to the axis Z (Fig. 3).

This comparison criterion is selected based on the fact that the poloidal motion of the liquid in a closed cavity can be caused only by vortex forces. The vertical forces cause vertical motion of the metal and the higher vorticity of these forces, the more intense the poloidal flow. In view of the foregoing, intensity of vorticity of the velocity field is qualitatively determined by volume-mean square vorticity of the vertical electromagnetic force

$$\Omega = \left| \sqrt{\frac{1}{V} \int_{V} \left\{ \left(\frac{\partial f_z}{\partial y} \right)^2 + \left(\frac{\partial f_z}{\partial x} \right)^2 \right\} dV} \right|, \quad (1)$$

where f_z — the vertical component of the electromagnetic force, V — the volume of the "warm top" with liquid aluminum (of the conducting cylinder) in the MHD stirrer.

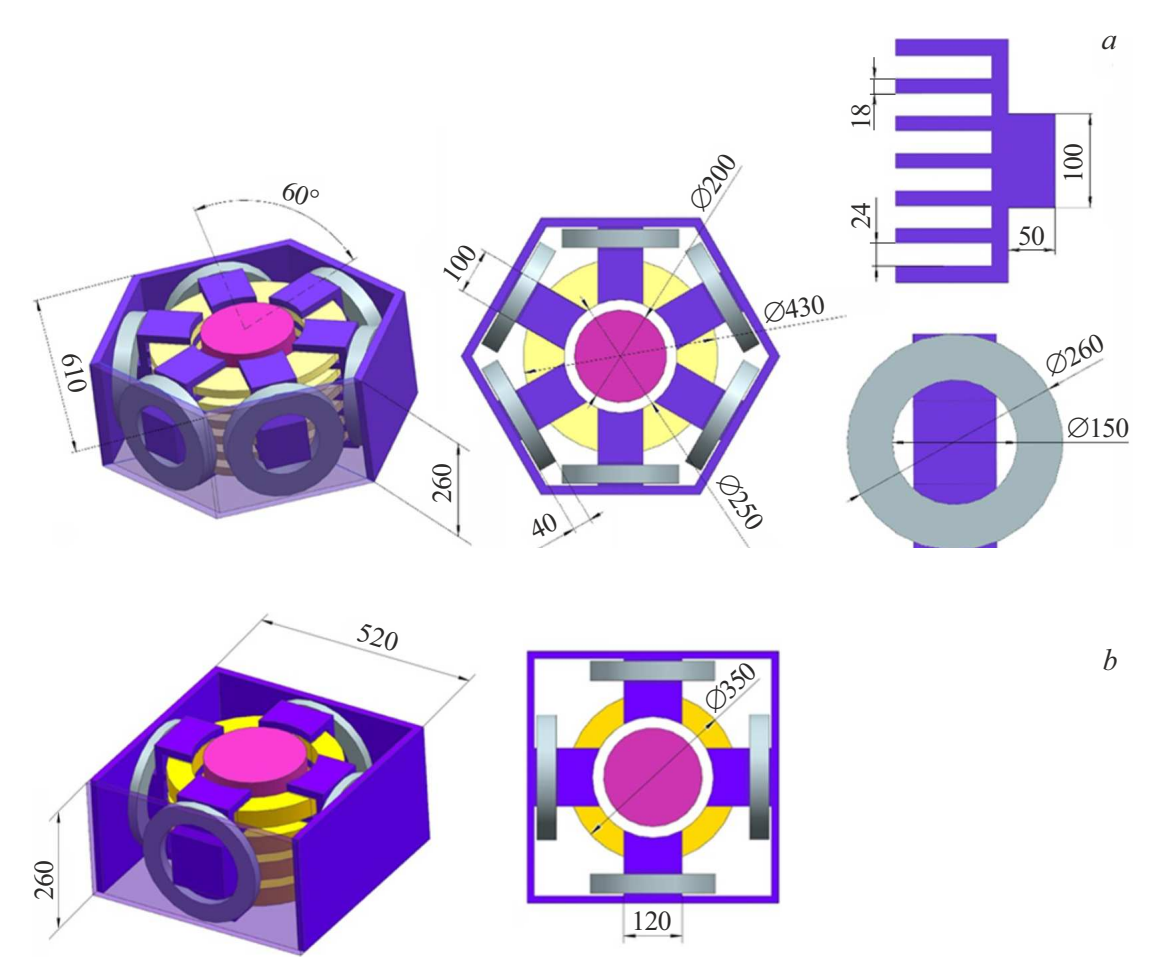


Figure 2. Layout of the three-phase (initial) (a) and the two-phase (b) variant of the MHD stirrer.

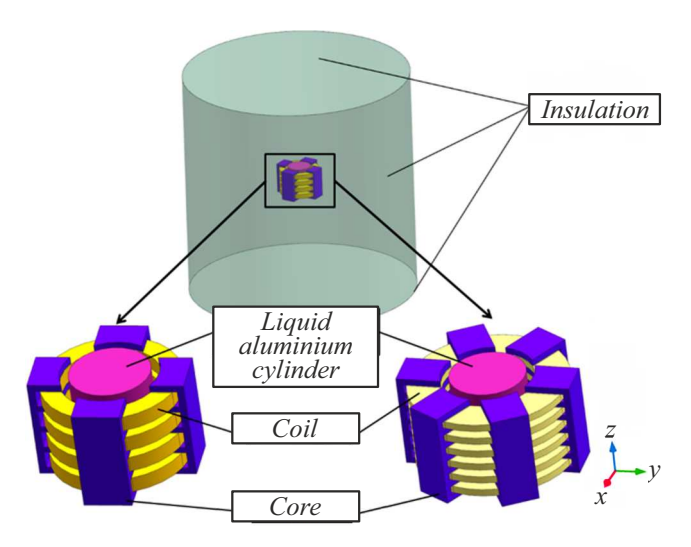


Figure 3. Computational model of the travelling field MHD inductor that includes poles with combs.

Within the framework of this comparison, numerical calculation was carried out in electrodynamic formulation without modeling hydrodynamic phenomena.

An important factor of stirring efficiency is distribution of local vorticity of the electromagnetic forces within the volume of the stirred liquid as well.

Formulation of the problem of calculation of the volume forces

Fig. 3 shows a simplified computational model of the travelling magnetic field's MHD stirrer. It consists of the core, the inductance coils, the liquid aluminum cylinder (only a liquid metal domain is modelled without taking into account container walls) and the external region. The numerical model is considered only in the electrodynamic formulation and solved in the Comsol Multiphysics 6.0 software package with defining the following boundary conditions [15–17]:

— the entire computational domain except for the inductance coils has a Maxwell system of equations solved in the low-frequency formulation; while it is assumed that the magnetic field varies in time according to a harmonic

law [15]:

$$\begin{cases}
\mathbf{E} = -i\omega\mathbf{A}, \\
\nabla \times \mathbf{H} = \mathbf{J}, \\
\mathbf{B} = \nabla \times \mathbf{A}, \\
\mathbf{J} = \sigma \mathbf{E}, \\
\operatorname{div} \mathbf{B} = 0,
\end{cases}$$
(2)

$$\mathbf{B} = \mu_0 \mu_r \mathbf{H},\tag{3}$$

where ${\bf H}$ — the vector of magnetic field strength, σ — the electrical conductivity of the material, ${\bf J}$ — the vector of common current density, ${\bf E}$ — the vector of electric field strength, ${\bf A}$ — the vector potential, ${\bf B}$ — the vector of magnetic field's magnetic induction, i — the imaginary unit, μ_0 — the permeability of vacuum, μ_r — the relative permeability of the material;

— an external boundary of the computational domain has a condition of "insulation" of the magnetic field defined (Magnetic Insulation):

$$\mathbf{n} \times \mathbf{A} = 0$$
,

where \mathbf{n} — the surface normal of the computational domain boundary.

— no induced vortex current in the core of the considered model is determined by defining extremely low electrical conductivity of the core material $(10^{-5}\,\mathrm{S/m})$, which does not affect distribution of the magnetic field, but improves stability of the solution unlike the case of zero conductivity.

— a homogenized model of calculation of the coils [16] with defining the current density without taking into account a geometry of a wound wire. The computational domain is a cylinder, whose cross-sectional area coincides with a winding cross-sectional area. The current density in the coil is determined by defining a number of coil turns and an amplitude value of the electric current in one turn (4). The current in the coils varies according to the harmonic law with taking into account a respective phase angle between the adjacent coils (90° in the two-phase variant and 60° in the three-phase variant);

$$\mathbf{J_e} = \frac{NI_{coil}}{A} \mathbf{e}_{coil},\tag{4}$$

where N — the number of coil turns, I_{coil} — the amplitude value of current in one turn, A — the cross-sectional area of the coil, \mathbf{e}_{coil} — the vector indicating a direction of current flow in the coil;

— the equations were solved in a fully coupled method, wherein all the differential equations are solved within the framework of one iteration with a direct solver (MUMPS) [17];

— the above-mentioned equations were solved in a Cartesian system of coordinates, whose origin coincides with a cylinder center and the axis z is co-directional to its axis.

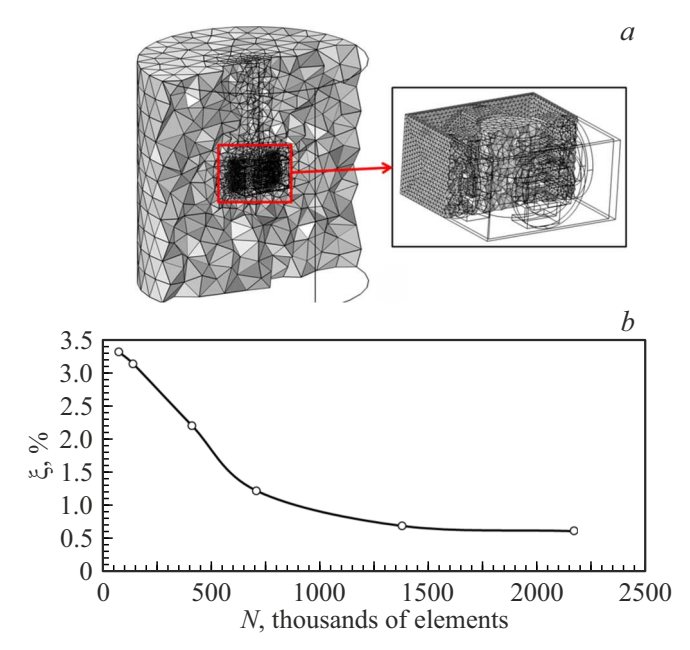


Figure 4. Grid model of the two-phase stirrer with the travelling magnetic field inductor (a); the graph of grid convergence, which shows dependence of accuracy of calculation of the electromagnetic force ξ on the number of elements of the grid model (b).

Fig. 4, a shows discretization of the computational domain as exemplified by the two-phase inductor stirrer. The present study investigated grid convergence, whose graph is shown on Fig. 4, b. Computational modeling of a considered item included assuming a tetrahedron grid model with 0.729 million elements, which corresponds to accuracy of grid convergence of the electromagnetic force of about 1% (this accuracy corresponds to the set goals and does not require substantial computing resources).

5. Results of computational modeling of the three-phase and two-phase travelling magnetic field inductors

Fig. 5 shows distribution of the induced electromagnetic force in a vertical section of the liquid metal volume as created by the two-phase and three-phase travelling field inductors of the MHD stirrer. The comparison was carried out at the magnetic field's maximum value of 20 mT inside the volume of the liquid metal.

Fig. 6 shows distribution of the *z*- component of the electromagnetic force on an external surface of the liquid metal conducting cylinder for the case of the two-phase and the three-phase inductor. By analyzing the figures 5 and 6, it can be noted that the forces having the maximum value are generated in the ingot opposite to the inductor poles, while its largest value is achieved in the two-phase inductor. Distribution of the force in the three-phase inductor is

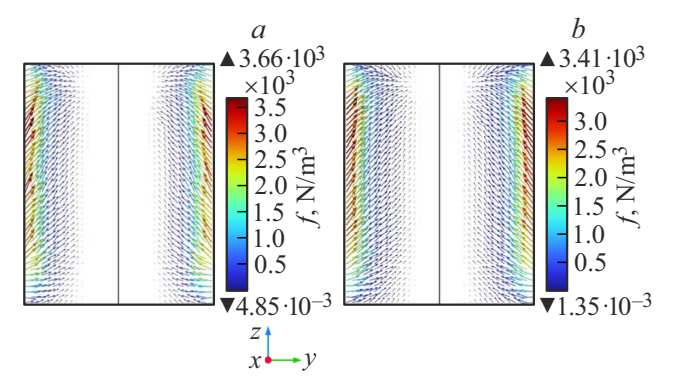


Figure 5. Distribution of the volume forces in the section of the liquid metal ingot of the two-phase (a) and three-phase (b) stirrers.

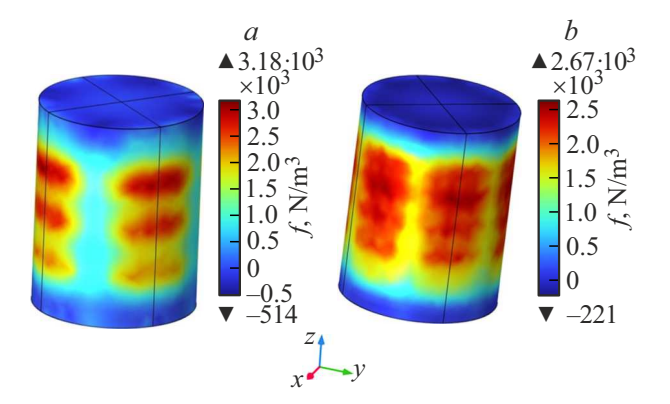


Figure 6. Distribution of the vertical component of the volume force within the volume of the liquid metal ingot with the two-phase (a) and the three-phase (b) inductor.

although lower by the maximum value, but totally it is higher across the whole volume, which is explained by more uniform distribution of the forces due to a larger number of the core poles (see Fig. 6 and Table).

Thus, in terms of vorticity of the electromagnetic forces the three-phase travelling field inductor is more effective than the two-phase travelling field inductor. In some cases, application of the two-phase inductors allows reducing the overall dimensions of the stirrer, thereby making it possible to fit into required sizes of a casting installation, but it will require increase of energy costs. For example, one can amplify the value of the magnetic field or enhance vorticity of the electromagnetic forces, which can be done by increasing the frequency of feeding electric current. When increasing the frequency of feeding electric current, a thickness of penetration of alternating magnetic field into the metal is reduced and, therefore, there is increase of nonuniformity of distribution of the electromagnetic forces along the radius from the surface deep into the liquid cylinder, thereby resulting in increase of vorticity of the forces.

5.1. Comparison of the two-phase rotating magnetic field inductor with the three-phase inductor

Fig. 7 shows simplified layouts of the three-phase travelling field inductor and the two-phase rotating field inductor, which are computational models.

When a rotational (toroidal) flow of the liquid is excited by the rotating magnetic field in the cylindrical cavity, even with intense rotation its vorticity is focused in a narrow boundary layer near the cavity walls and at the crystallization front, while in a nucleus the liquid is rotated like a solid body. The flow can be brought to azimuthal rotation by forces, whose axial component of the rotor is zero. Therefore, the three-phase rotating field inductor and the two-phase rotating field inductor can be compared by a value of the axial component of a specific moment of the volume electromagnetic forces, which is created by these inductors and defined as follows

$$\mathbf{M} = \mathbf{f} \times \mathbf{r} = \begin{vmatrix} \mathbf{i} & \mathbf{j} & \mathbf{k} \\ f_x & f_y & f_z \\ r_x & r_y & r_z \end{vmatrix} = (f_y r_z - f_z r_y) \mathbf{i}$$

$$+ (f_z r_x - f_x r_z) \mathbf{j} + (f_x r_y - f_y r_x) \mathbf{k},$$
(5)

where \mathbf{r} — the radius vector outgoing from the cylinder center; \mathbf{f} — the vector of the volume electromagnetic force; \mathbf{M} — the vector of the moment of the electromagnetic forces in a point; r_x , r_y , r_z , f_x , f_y , f_z — the components of the respective vectors in the Cartesian system of coordinates.

In order to analyze efficiency of stirring due to effect of the rotating magnetic field that is created by the considered MHD stirrers, a volume-averaged component of the full moment that ensures rotation of the liquid in relation to the cylinder axis (in this problem formulation - in relation of the axis z which coincides with the cylinder axis) was compared.

A value of the volume-averaged z component (along the cylinder axis) of the moment of the volume forces is determined as

$$\overline{M_z} = \frac{\int\limits_V (f_x r_y - f_y r_x) dV}{V}.$$
 (6)

6. Results of computational modeling of the three-phase and two-phase rotating magnetic field inductors

In this case the problem formulation is similar to the problem formulation for calculating the travelling field stirrer, with the only difference that the coils are arranged so that a coil axis is perpendicular to the axis of the conducting cylinder. The axes of all the coils are in a plane of a central horizontal section of the cylinders and are circumferentially spaced by a value of the phase angle (in the two-phase and three-phase inductors it is 90° and 60°, respectively).

Parameter	Two-phase travelling field stirrer	Three-phase travelling field stirrer	Two-phase rotating field stirrer	Three-phase rotating field stirrer
B_{\max}, T	0.0204	0.0204	0.0205	0.0218
$'\Omega, N/m^4$	1430	2940	_	_
$f_z^{\text{max}}, \text{N/m}^3$	2850	2540	_	_
$f_{\varphi}^{\text{max}}, \text{N/m}^3$	_	-	4430	4380
$\overline{M_z}$, N/m ²	_	_	16.64	33.5

Characteristics of the considered layouts of the MHD stirrers

Fig. 8 shows distribution of the induced electromagnetic force in the section of the liquid metal ingot. It can be noted that distribution of the maximum force is in the narrow boundary layer near the cylinder walls in the case of the two-phase and the three-phase inductor.

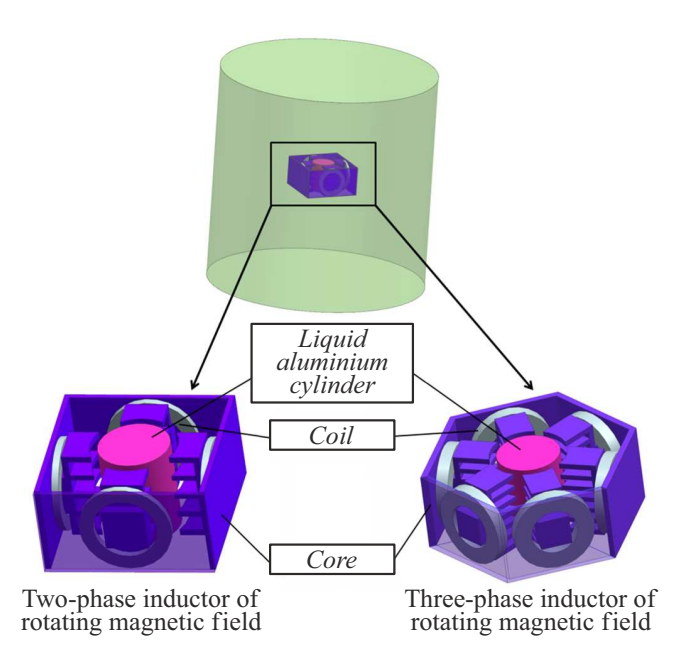


Figure 7. Computational model of the rotating magnetic field inductors in the Cartesian system of coordinates, which is similar to the system shown in Fig. 3 and is not shown in this figure.

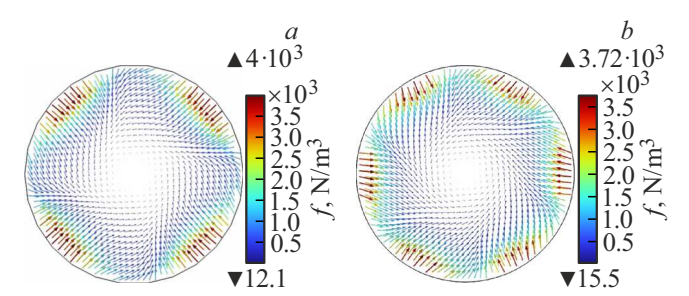


Figure 8. Distribution of the electromagnetic volume force in the section of the liquid metal cylindrical volume; a — the two-phase rotating field inductor, b — the three-phase rotating field inductor.

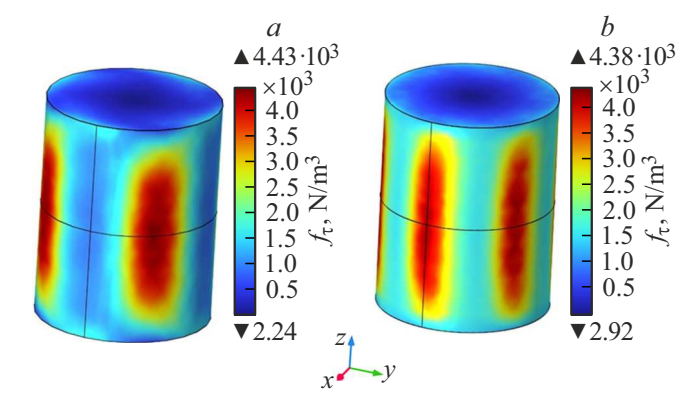


Figure 9. Distribution of the azimuthal component of the volume forces (f_{τ}) in the liquid metal for the two-phase (a) and three-phase (b) rotating field inductors.

The distribution of the force within the volume is concentrated in the liquid metal domain opposite to the cores, which means that with an equal value of the maximum volume force the specific value of the moment of the volume forces will be higher in the three-phase inductor variant (see Fig. 9 and Table).

Results given in the table have been analyzed to show that the MHD stirrers that combine the travelling and rotating magnetic field inductors in the three-phase variant have parameters which are better than those of the two-phase MHD stirrers. However, in some cases, when the small sizes of the structure are a crucial factor, reduction of the dimensions of the stirrer by using the two-phase inductor may be critical, wherein differences in characteristics can be mitigated by increasing the value of the magnetic field or increasing its frequency.

Rotating magnetic field inductor with the inclined cores

It is possible to substantially reduce the overall dimensions of the MHD stirrer by omitting the travelling field inductor. At the same time, it is necessary that the only remaining rotating magnetic field inductor can create not only toroidal rotation of the liquid, but would create flows

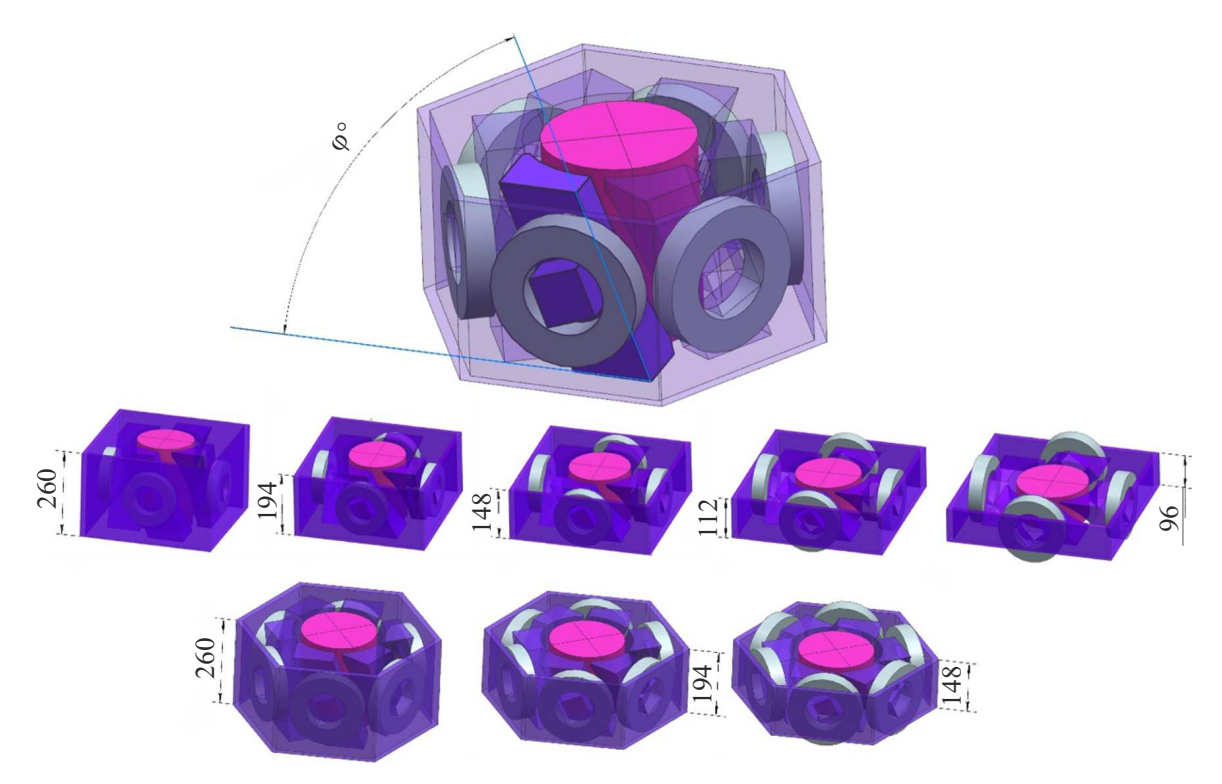


Figure 10. Geometry of the rotating field stirrer with the inclined cores.

in a vertical plane. One of the variants may be a rotating field inductor with cores inclined in relation to the central axis of the stirrer in a plane that is parallel to the plane of its longitudinal section (Fig. 10).

Fig. 10 shows the geometry of the (two-phase and three-phase) stirrer with vertical overall dimensions depending on a value of the inclination angle of the core. Due to structural limitations, only the angles φ 20°, 25°, 30°, 35° and 40° for the two-phase inductor have been considered, so have the angles φ 20°, 25° and 30° for the three-phase inductor. This design was obtained by inclining the pole while keeping its original width. Coils of this design are connected similar to a diagram of the rotating magnetic field inductors. In the liquid metal within the working volume of the MHD stirrer, the alternating rotating magnetic field induces an electric current, whose line form near the core poles can be represented as closed elongated loops that reproduce a form of the poles and their inclination (Fig. 11, a).

The induced current interacts with the rotating magnetic field within the working volume and the liquid metal originates a volume force f that is directed normally to lines of the electric current (Fig. 11, b). This force has both the vertical f_z and the horizontal f_φ components, which is confirmed by a computational experiment.

This stirrer design creating simultaneously toroidal and poloidal stirring of the liquid metal has not an additional travelling field inductor. As a result of this, the stirrer

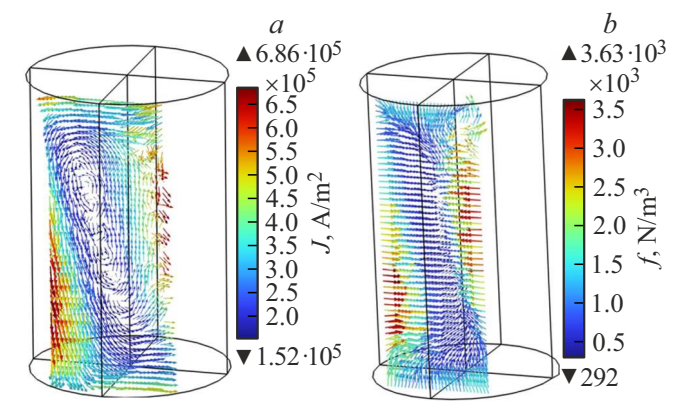


Figure 11. Vectors of the electric current in a section of the liquid metal cylinder (a); vectors of the volume electromagnetic force (b).

structure has dimensions that are less than structures of its prototypes.

The parameters taken by us above were used to compare efficiency of the described design creating both the forces rotating the liquid metal and the forces causing its vertical motion with the designs of the MHD stirrers that have two inductors of both travelling and rotating fields.

The problem formulation for calculation of the rotating field MHD stirrer with the inclined cores was similar to the above-described variant and therefore it is not given below.

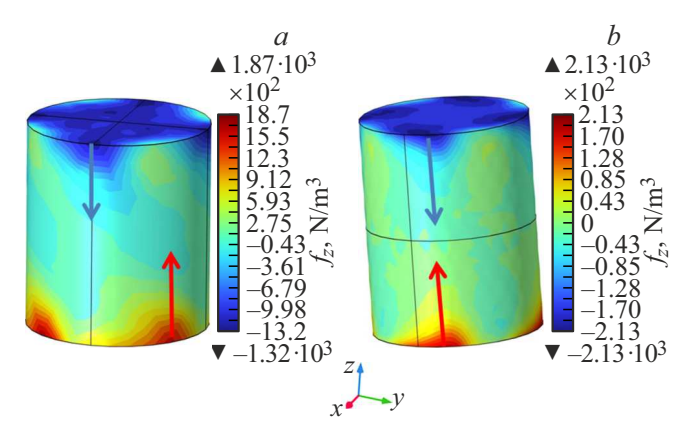


Figure 12. Distribution of the vertical component of the volume force in the two-phase rotating field MHD stirrer with the inclined cores (a) and the two-phase rotating field MHD stirrer without inclination of the cores (b).

Results of computational modeling of the three-phase and two-phase rotating field inductors with the inclined cores

Fig. 12 shows distribution of the vertical component of the force across the surface of the conducting cylinder of the two-phase rotating field MHD stirrer with the inclined cores as compared to the similar variant without inclination.

As said above, the vertical forces that generally determine the poloidal flow are created by interaction of the rotating magnetic field with its induced electric current in the cylinder. However, analysis of Fig. 12 shows that when using the inclined cores, concentrations of the vertical components of the force, which occur at an upper and a lower boundary of the conducting ingot due to an edge effect, are shifted aside in relation to each other, which also contributes to formation of vortex motion of the liquid metal in the vertical plane. Without inclination of the core

poles, the rotating field creates only a tangential component of the electromagnetic forces, while forces caused by the edge effects are counter directed, which does not allow for generation of a large vortex.

The present study has numerically investigated the dependences of our used characteristics of the electromagnetic forces that create the vertical flows on the inclination angle of the poles of the rotating magnetic field inductor of the MHD stirrer (Fig. 13). Below are graphs of the dependence of the maximum specific vertical electromagnetic force that acts within the liquid metal volume on the inclination angle of the core poles and of the dependence of the mean-square rotor of the electromagnetic forces on the same.

By analyzing the obtained graphs, it can be concluded that the dependence of the maximum vertical component of the electromagnetic force on the inclination angle of the core poles has a pronounced maximum in both variants of the considered designs (Fig. 13, a). It indicates that in terms of the maximum force that creates the poloidal flow there is the best inclination angle of the pole, which corresponds to the most effective operation of the inductor. It is useful to take it into account when designing these devices. The dependence of the mean-square vorticity of the volume force Ω on the inclination angle of the core poles (Fig. 13, α) is analyzed to show that the considered variants are less efficient than the stirrers that contain the travelling field inductor, but are not far away from them in terms of generability of the poloidal flow.

Conclusion

The study has analyzed the various variants of designs of the MHD stirrers and identified advantages and disadvantages of each design. More complete investigation in this field requires considering a hydrodynamic part of the set problem. The considered variants of the stirrers with the three-phase rotating and travelling magnetic fields inductors exceed the two-phase inductors by a created

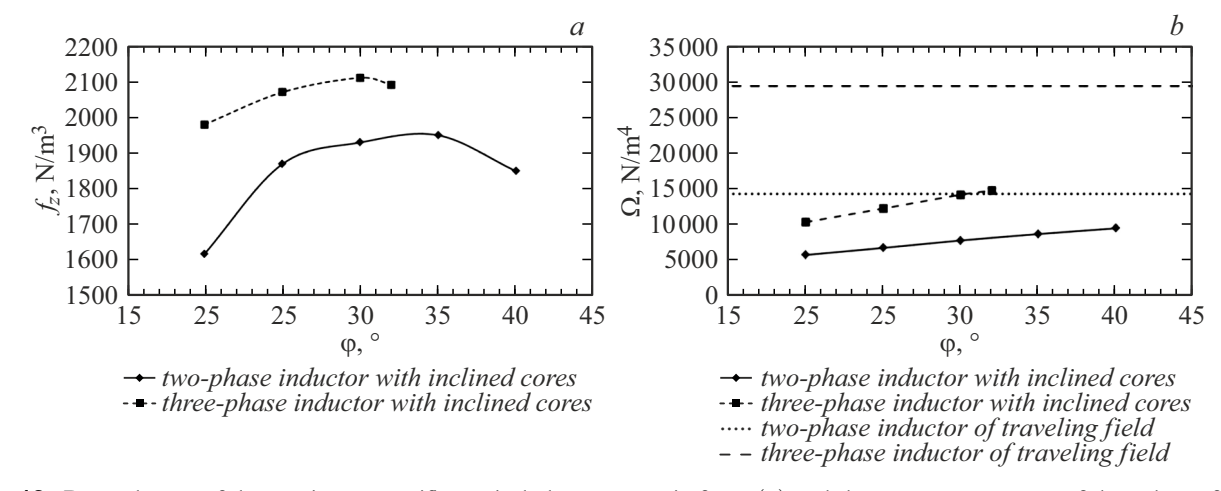


Figure 13. Dependences of the maximum specific vertical electromagnetic force (a) and the mean-square rotor of the volume force (b) on the inclination angle of the core poles.

moment of the forces that rotate the liquid metal and by vorticity (created by the travelling magnetic field) of the electromagnetic forces that create poloidal motion of the liquid metal. At the same time, the magnitudes of the volume electromagnetic forces that are created in the liquid metal by the three-phase and the two-phase MHD stirrers have close values. Application of the two-phase rotating magnetic field inductors will require increase of the feeding electric power in comparison with the three-phase inductors. But it can be justified due to the fact that they are smaller in overall dimensions and it is more easy to combine them with other similar cores into a single system which will have smaller overall dimensions than the system of the independent three-phase stirrers.

The paper has proposed and studied a fundamentally new diagram of the MHD stirrer with the inductor that has inclined core poles, which has not the travelling field inductor and is designed to create both the toroidal and the vertical stirring flows within the stirred volume of the metal.

Funding

This study was carried out in accordance with fiscal plan of the Institute of Continuous Media Mechanics (Ural Branch, Russian Academy of Sciences) Large-scale flows and heat exchange in the conducting and the non-conducting liquid in conditions of small-scale turbulence N_2 124012300246-9.

Conflict of interest

The authors declare that they have no conflict of interest.

References

- [1] V.G. Borisov. Light Alloy Technol., **50** (2), 48 (2016).
- [2] C. Mapelli, A. Gruttadauria, W. Peroni. J. Mater. Processing Technol., 210 (2), 306 (2010).
 DOI: 10.1016/j.jmatprotec.2009.09.016
- [3] V.G. Borisov. Metallurgist, 52 (11-12), 672 (2008).
- [4] Yu.M. Gelfgat, Yu. Krumins, M. Abricka. Magnetohydrodynamics, 35 (1), 1 (1999).
- [5] S. Denisov, V. Dolgikh, S. Khripchenko, I. Kolesnichenko, L. Nikulin. Magnetohydrodynamics, 50 (4), 407 (2014).
- [6] A.Yu. Vasil'ev, I.V. Kolesnichenko, A.D. Mamykin, P.G. Frik, R.I. Khalilov, S.A. Rogozhkin, V.V. Pakholkov. ZhTF, 85 (9), 45 (2015) (in Russian).
- [7] S. Yu. Khripchenko. J. Engineer. Phys. Thermophys., 95 (5), 1126 (2022). DOI: 10.1007/s10891-022-02577-w
- [8] B. Willers, S. Eckert, P. A. Nikrityuk, D. Räbiger, J. Dong, K. Eckert, G. Gerbeth. Metall. Mater. Trans. B, 39B, 304 (2008).
- [9] D. Rabiger, S. Eckert, G. Gerbeth, S. Franke, J. Czarske. Magnetohydrodynamics, 48 (1), 213 (2012).
- [10] S. Khripchenko, S. Denisov. Magnetohydrodynamics, 56 (4), 427 (2020). DOI: 10.22364/mhd.56.4.1
- [11] J. Stiller, K. Koal, W.E. Nagel, J. Pal, A. Cramer. Eur. Phys. J. Special Topics, 220, 111 (2013).

- [12] M.Yu. Kuchinskii. Elektrotechnologiya peremeshivaniya zhidkoi serdtseviny slitkov v mnogoruch'evom liteinom komplekse (Kand. diss., Krasnoyarsk, 2022), 103 s. (in Russian).
- [13] M.V. Pervukhin, M.Yu. Kuchinskii, S.P. Timofeev. Zhurnal SFU. Tekhnika i tekhnologii, **12** (8), 952 (2019) (in Russian).
- [14] S.Yu. Khripchenko, V.G. Borisov. Ustroistvo dlya peremeshivaniya elektroprovodnykh zhidkikh sred. (Pat. № 2830293 Zayavka № 2024118853 Prioritet izobreteniya 04 iyulya 2024 g. Gos. registratsiya 18 noyabrya 2024 g.) (in Russian).
- [15] E. Shvydkiy, V. Zaharov, K. Bolotin, I. Smolyanov, S. Sarapulov. Magnetohydrodynamics, 53 (4), 707 (2017).
- [16] C.R. Vargas-Llanos, F. Huber, N. Riva, M. Zhang, F. Grilli. Superconductor Sci. Technol., 35, 41 (2022).
- [17] N.E. Jewell-Larsen, S.V. Karpov, I.A. Krichtafovitch, V. Jayanty, Ch.-P. Hsu, A.V. Mamishev. ESA Annual Meeting on Electrostatics, 1, 20 (2008).

Translated by M.Shevelev